Electronic Supplementary Material (ESI) for Materials Chemistry Frontiers.

Electronic supplementary information (ESI) for

$LiRE(SO_4)_2$ (RE = Y, Gd, Eu): noncentrosymmetric chiral rare-earth sulfates with very large band gaps

*Sunghwan Cho and Kang Min Ok**

Department of Chemistry, Sogang University, Seoul 04107, Republic of Korea

*E-mail: kmok@sogang.ac.kr

Table of contents

Table S1. Selected bond distances (Å) of $LiY(SO_4)_2$.

Li(1)-O(2)	1.9172(15)
Y(1)-O(1)	2.2921(16)
Y(1)-O(2)	2.4449(14)
S(1)-O(1)	1.4622(16)
S(1)-O(2)	1.4839(15)

Table S2. Selected bond distances (Å) of $LiGd(SO_4)_2$.

Li(1)-O(2)	1.9332(16)
Gd(1)-O(1)	2.3312(18)
Gd(1)-O(2)	2.4774(16)
S(1)-O(1)	1.4634(18)
S(1)-O(2)	1.4862(16)

Table S3. Selected bond distances (Å) of $LiEu(SO_4)_2$.

Li(1)-O(2)	1.9378(18)
Eu(1)-O(1)	2.342(2)
Eu(1)-O(2)	2.4881(18)
S(1)-O(1)	1.462(2)
S(1)-O(2)	1.4857(18)

Table S4. Selected bond angles (°) of $LiY(SO_4)_2$.

O(2)-Li(1)-O(2)	100.24(4)	O(1)-Y(1)-O(1)	151.73(8)
O(2)-Li(1)-O(2)	130.12(10)	O(1)-Y(1)-O(2)	83.12(6)
O(1)-S(1)-O(1)	109.88(14)	O(1)-Y(1)-O(2)	130.40(5)
O(1)-S(1)-O(2)	111.47(9)	O(1)-Y(1)-O(2)	77.35(6)
O(1)-S(1)-O(2)	110.12(10)	O(1)-Y(1)-O(2)	71.96(6)
O(2)-S(1)-O(2)	103.66(11)	O(2)-Y(1)-O(2)	130.60(7)
O(1)-Y(1)-O(1)	101.52(9)	O(2)-Y(1)-O(2)	153.38(8)
O(1)-Y(1)-O(1)	85.38(9)	O(2)-Y(1)-O(2)	57.00(7)

Table S5. Selected bond angles (°) of $LiGd(SO_4)_2$.

O(2)-Li(1)-O(2)0	100.21(4)	O(1)-Gd(1)-O(1)	102.13(9)
O(2)-Li(1)-O(2)	130.21(11)	O(1)-Gd(1)-O(2)	130.27(6)
O(1)-S(1)-O(1)	110.08(15)	O(1)-Gd(1)-O(2)	77.60(6)
O(1)-S(1)-O(2)	111.18(10)	O(1)-Gd(1)-O(2)	72.28(6)
O(1)-S(1)-O(2)	110.00(11)	O(1)-Gd(1)-O(2)	82.69(6)
O(2)-S(1)-O(2)	104.27(13)	O(2)-Gd(1)-O(2)	56.53(7)
O(1)-Gd(1)-O(1)	151.63(9)	O(2)-Gd(1)-O(2)	131.21(7)
O(1)-Gd(1)-O(1)	84.83(9)	O(2)-Gd(1)-O(2)	153.21(9)

Table S6. Selected bond angles (°) of $LiEu(SO_4)_2$.

O(2)-Li(1)-O(2)	100.40(5)	O(1)-Eu(1)-O(1)	102.51(10)
O(2)-Li(1)-O(2)	129.72(13)	O(1)-Eu(1)-O(2)	77.65(7)
O(1)-S(1)-O(1)	109.93(17)	O(1)-Eu(1)-O(2)	129.98(7)
O(1)-S(1)-O(2)	111.07(12)	O(1)-Eu(1)-O(2)	82.75(7)
O(1)-S(1)-O(2)	110.11(12)	O(1)-Eu(1)-O(2)	72.41(7)
O(2)-S(1)-O(2)	104.45(14)	O(2)-Eu(1)-O(2)	56.33(8)
O(1)-Eu(1)-O(1)	151.87(10)	O(2)-Eu(1)-O(2)	131.29(8)
O(1)-Eu(1)-O(1)	84.35(10)	O(2)-Eu(1)-O(2)	153.46(10)

Table S7. Bond valence sum calculations for $LiRE(SO_4)_2$ (RE = Y, Gd, Eu).

$LiY(SO_4)_2$		**$LiGd(SO_4)_2$**		**$LiEu(SO_4)_2$**	
Li1	1.18	Li1	1.13	Li1	1.12
Y1	3.13	Gd1	3.26	Eu1	3.24
S1	6.02	S1	5.99	S1	6.01
O1	2.02	O1	2.03	O1	2.06
O2	2.07	O2	2.06	O2	2.04

Table S8. Atomic coordinates (Å) and equivalent isotropic displacement parameters (Å^2) for $LiY(SO_4)_2$.

	Wyck.	*x*	*y*	*z*	*U*(eq)
Li(1)	2b	0.5	0.5	1	0.0143(17)
Y(1)	2d	0.5	0	0.25	0.00650(14)
S(1)	4f	0.28622(5)	0.21378(5)	0.75	0.00718(16)
O(1)	8i	0.4169(2)	0.1876(2)	0.5571(3)	0.0149(3)
O(2)	8i	0.29599(19)	0.3948(2)	0.8526(3)	0.0109(3)

U(eq) is defined as one third of the trace of the orthogonalized U^{ij} tensor.

Table S9. Atomic coordinates (Å) and equivalent isotropic displacement parameters (Å^2) for $LiGd(SO_4)_2$.

	Wyck.	*x*	*y*	*z*	*U*(eq)
Li(1)	2b	0.5	0.5	1	0.016(2)
Gd(1)	2d	0.5	0	0.25	0.00723(9)
S(1)	4f	0.28662(6)	0.21338(6)	0.75	0.00817(13)
O(1)	8i	0.4172(2)	0.1886(2)	0.5600(3)	0.0170(4)
O(2)	8i	0.2969(2)	0.3927(2)	0.8534(3)	0.0118(3)

U(eq) is defined as one third of the trace of the orthogonalized U^{ij} tensor.

Table S10. Atomic coordinates (Å) and equivalent isotropic displacement parameters (Å^2) for $LiEu(SO_4)_2$.

	Wyck.	*x*	*Y*	*z*	*U*(eq)
Li(1)	2b	0.5	0.5	1	0.016(2)
Eu(1)	2d	0.5	0	0.25	0.00732(11)
S(1)	4f	0.28692(6)	0.21308(6)	0.75	0.00821(15)
O(1)	8i	0.4171(3)	0.1881(3)	0.5612(4)	0.0174(4)
O(2)	8i	0.2976(2)	0.3921(2)	0.8524(4)	0.0118(3)

U(eq) is defined as one third of the trace of the orthogonalized U^{ij} tensor.

Figure S1. Calculated and experimental powder X-ray diffraction patterns of $LiRE(SO_4)_2$, (RE = Y, Ga, and Eu).

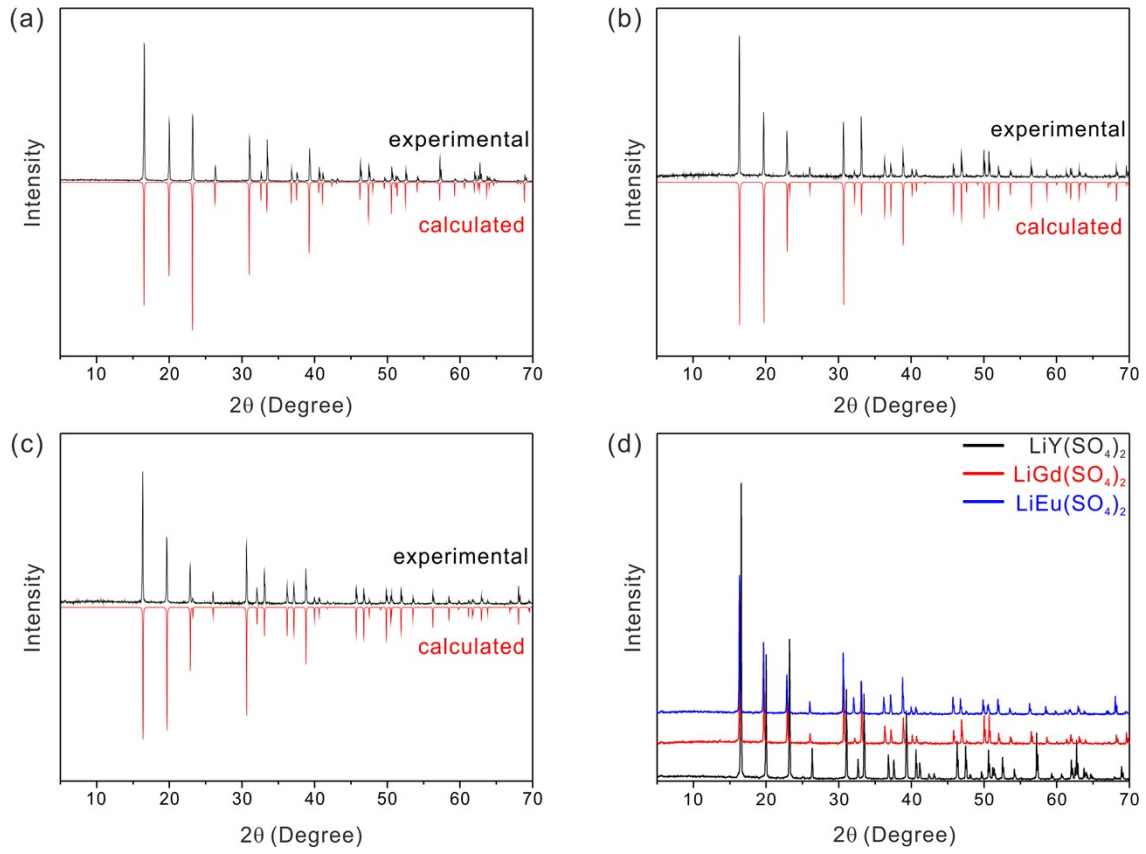

Figure S2. IR spectra of $LiRE(SO_4)_2$ (RE = Y, Gd, Eu).

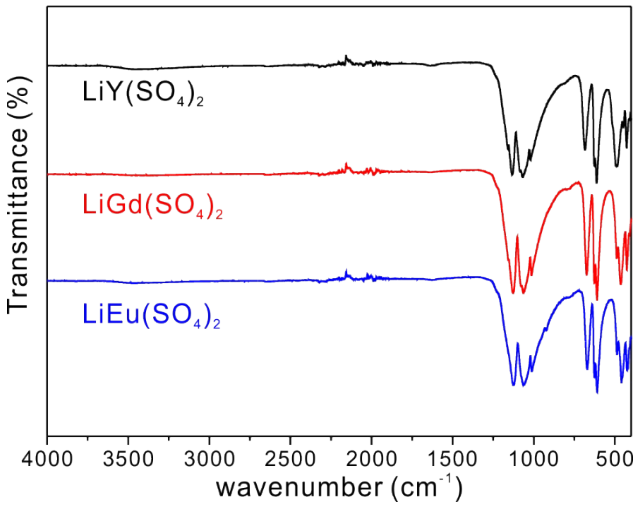

Figure S3. TGA diagrams of (a) $LiY(SO_4)_2$, (b) $LiGd(SO_4)_2$, and (c) $LiEu(SO_4)_2$.

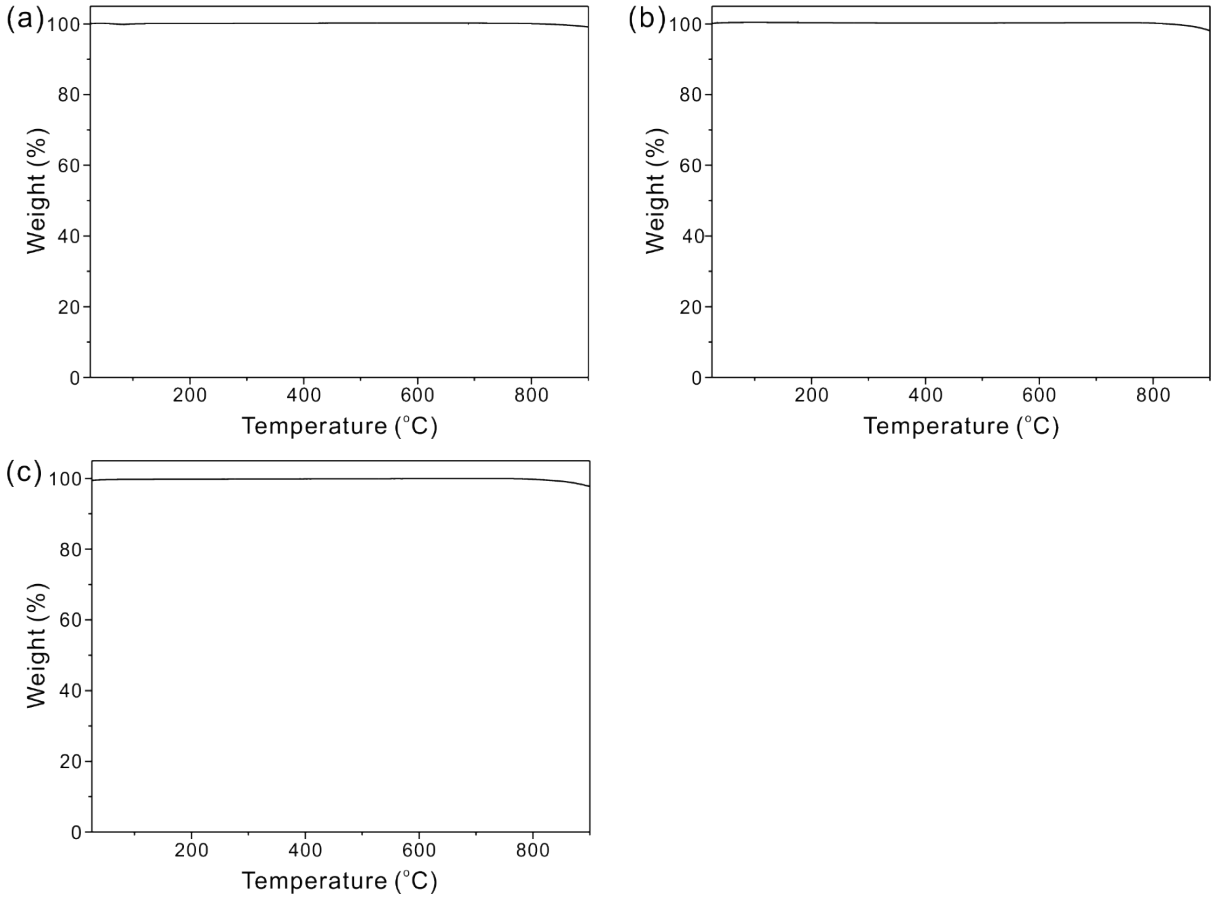

Figure S4. Powder X-ray diffraction patterns of (a) $LiY(SO_4)_2$, (b) $LiGd(SO_4)_2$, and (c) $LiEu(SO_4)_2$ after heating at 600 ℃, 650 ℃, and 820 ℃, respectively, for 24 h.

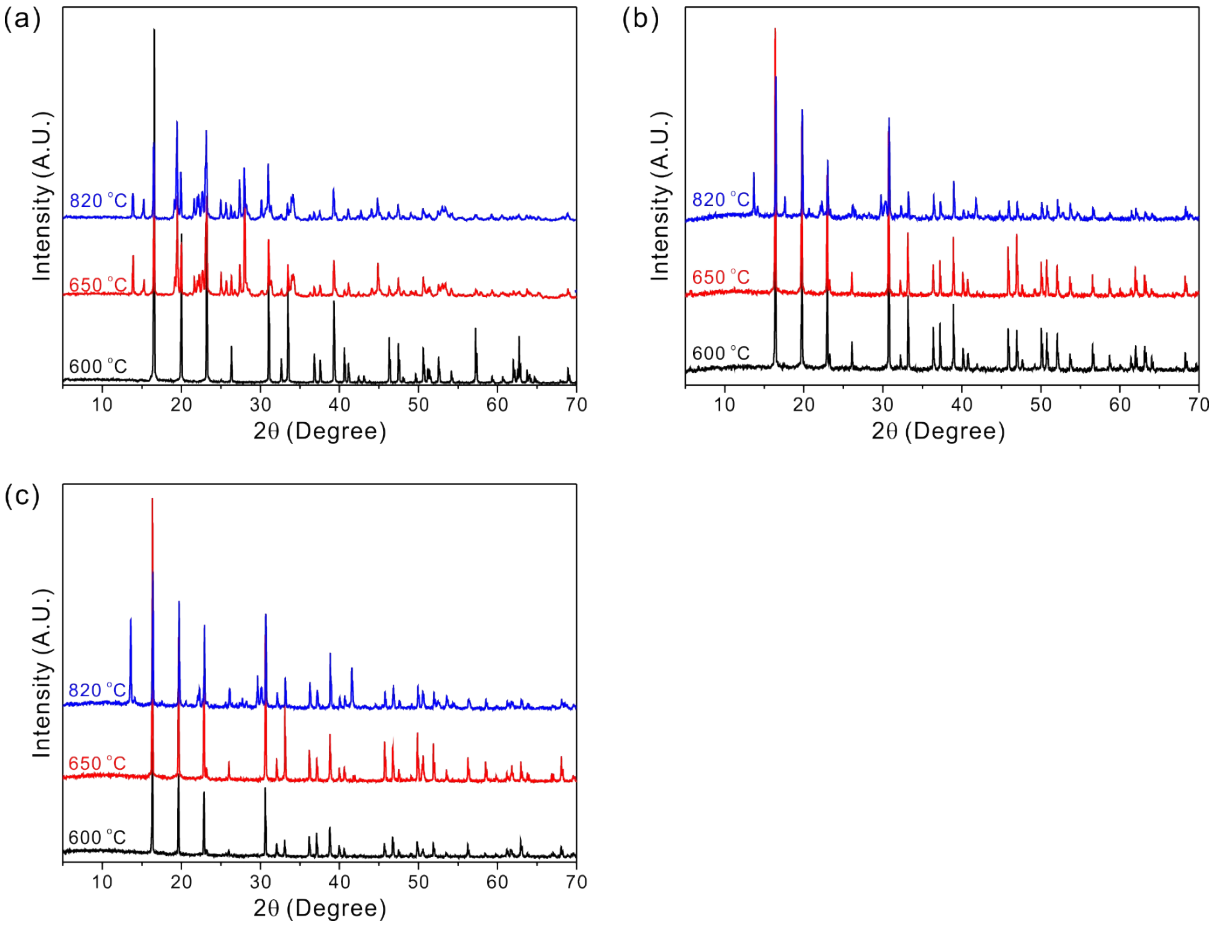

Figure S5. Powder X-ray diffraction patterns of (a), (b) $LiY(SO_4)_2$, (c), (d) $LiGd(SO_4)_2$, and (e), (f) $LiEu(SO_4)_2$ after heating at 1000 ℃ for 2h [(a), (c), (e)] and for 14h [(b), (d), (f)], respectively.

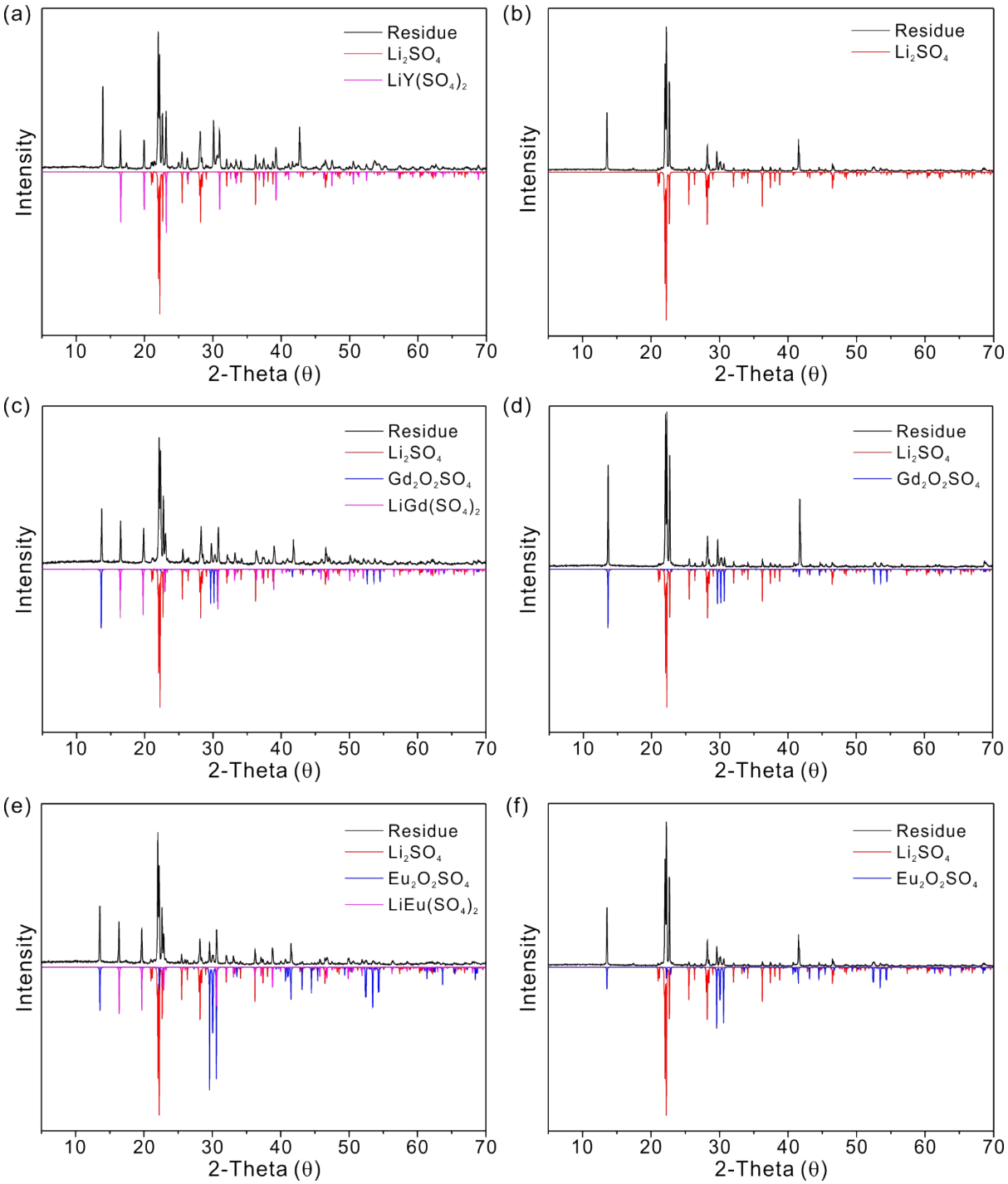

Peaks that are not assigned in (a) and (b) are supposed to be $Y_2O_2SO_4$, but its precise structural data were not reported.

Figure S6. Band structures of (a) $LiY(SO_4)_2$, (b) $LiGd(SO_4)_2$, and (c) $LiEu(SO_4)_2$.

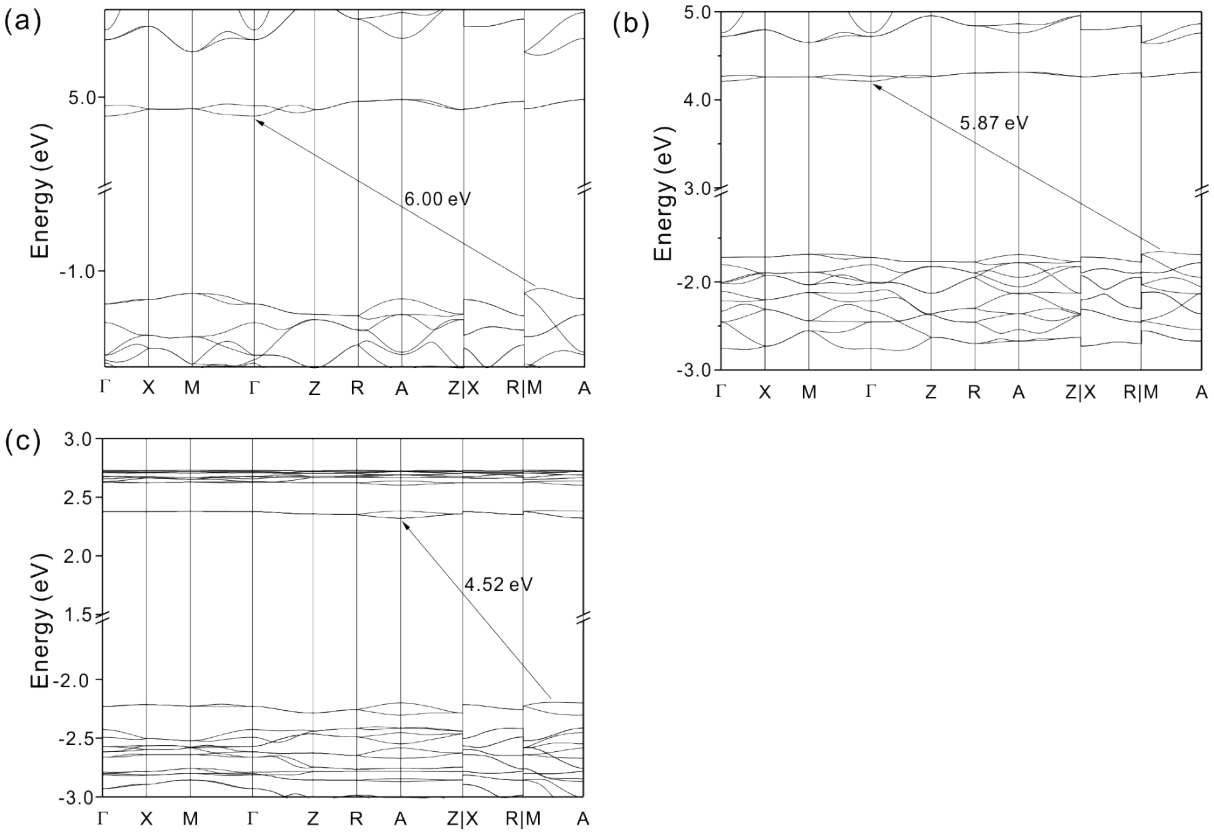

Figure S7. Total and partial density of states for (a) $LiY(SO_4)_2$, (b) $LiGd(SO_4)_2$, and (c) $LiEu(SO_4)_2$. The Fermi level is represented at 0 eV.